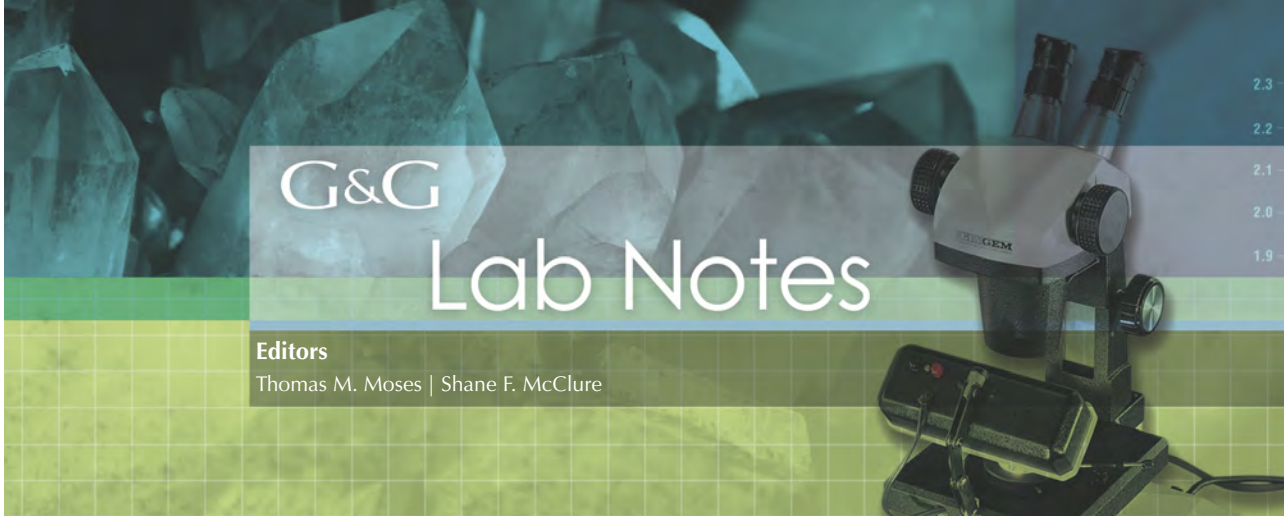

DIAMONDS

Evidence of Focused Beam Irradiation In Treated Pink Diamond

A Fancy pink diamond, confirmed as natural-grown, was found to be type IIa and colored by NV^- centers. As part of routine testing, DiamondView fluorescence images were collected to check for synthetic growth features. These images showed unusual patterning in the form of two pink spots near the edge of the table facet (figure 1). Both spots were approximately 0.9 × 0.7 mm, and the table facet was approximately 3.0 mm in diameter. The orange fluorescence throughout most of the table was likely due to NV^0 centers, whereas the pink components were likely due to NV^- centers.

To further investigate the spatial distribution of the $NV^0/^-$ centers, we acquired a photoluminescence (PL) image of the diamond's table using a 532 nm laser. Figure 2 shows the distribution of the NV^0 and NV^- centers. The distribution of the NV centers confirms the presence of two spots on the table. Figure 3 shows the average PL spectra from inside one of the spots and the average PL spectra from the region outside the spots. Figures 2 and 3 demonstrate that the intensity of the NV centers was greater inside the spots than in the rest of the table. Inside the spots, the average peak area intensity of the NV^0 center was approximately two times greater and the average peak area intensity of the NV^- centers was approximately three times greater. The spots were comparable in both size and defect concentrations.

To determine the vertical distribution of the NV^- center, a 500 µm PL depth profile was acquired through each spot. This is an automated process the instrument can perform in which a series of spectra are collected along a line spanning the diameter of the spot. The stage is then offset 5 µm in the vertical direction to focus farther into the diamond, and another series of spectra are collected. The process was repeated 100 times until the target depth of 500 µm was reached. This

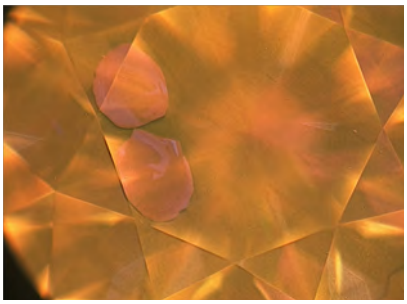

Figure 1. This DiamondView image of the table of a pink diamond shows two distinct pink spots. Field of view approximately 5 mm.

Figure 2. Left: A PL map showing the peak area distribution of the NV^0 center. Field of view is approximately 3 mm; scale is relative intensity. Right: A PL map showing the peak area distribution of the NV^- center. Field of view is approximately 3 mm; scale is relative intensity.

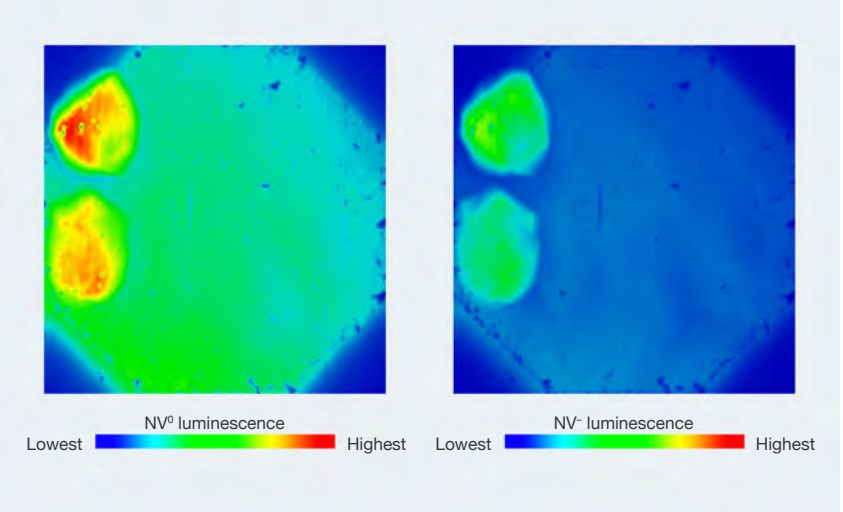

Editors' note: All items were written by staff members of GIA laboratories.

Gems & Gemology, Vol. 52, No. 2, pp. 298–309.

© 2016 Gemological Institute of America

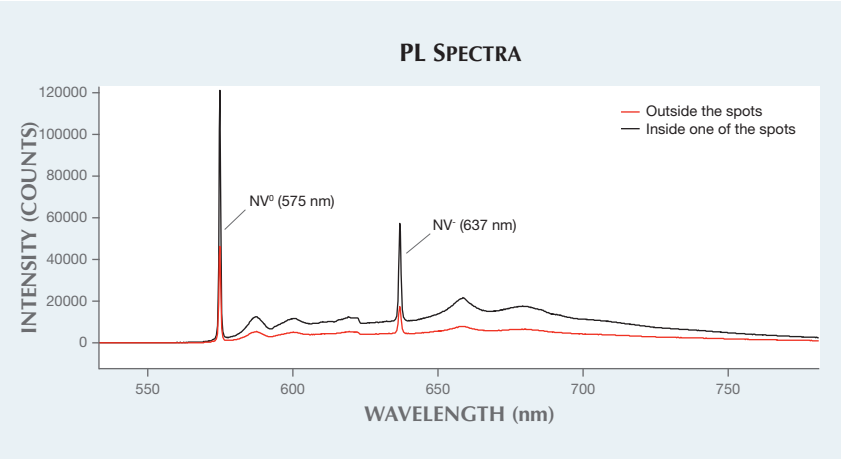

Figure 3. A comparison between average PL spectra from inside one of the spots and the area outside the spots. The y-axis scale is the same for both spectra, so it is apparent that the intensity inside the spot is higher for both NV^0 and NV^- centers.

achieved a depth profile of NV^- luminescence, indicating how deeply the irradiation beam had penetrated into the stone. One spot showed an average penetration depth of 100 µm and the other 50 µm. It is important to note that this is axial displacement, which in confocal microscopy is an approximation of the true depth of the illuminated feature. Nevertheless, this demonstrated the shallow penetration of the irradiation beam.

The intensity variation in the NV centers strongly demonstrated that this diamond was HPHT annealed and isolated nitrogen was subsequently introduced due to disaggregation of the A-form nitrogen (pairs of nitrogen atoms) or B-form nitrogen (four nitrogen atoms around a vacancy). It also indicated that this diamond was irradiated by a focused electron beam with relatively low energy (≤ 1 MeV) prior to annealing. These multiple processes introduced high concentrations of NV centers into the localized shallow areas. Furthermore, an increase of electron donor defects at the incident beam area would lead to the observed patterned distribution of the NV^- centers. The narrow, focused nature of the electron beam is responsible for the distribution of the defects into the two spots and therefore the reason why the pink spots are observed in the DiamondView image. The two spots may be the result of two separate beams in the irradiation setup. Alternatively, the second spot may be from an additional round of treatment designed to further enhance the color. It is also unusual for the treatment to be done through the table rather than on the culet. It is unknown what benefits the focused beam will have over wide-beam irradiation.

Troy Ardon and Lorne Loudin

Figure 4. This 4.29 ct type IIa color-treated diamond was graded as Fancy brown-pink under daylight conditions (left) and appeared Fancy purplish gray under incandescent lighting (right). The color change is due to strong NV fluorescence under UV to blue light exposure and irradiation-related GR1 absorption under incandescent illumination.

Treated Pink Type IIa Diamond Colored by Red Luminescence

Recently, the Carlsbad laboratory received a 4.29 ct type IIa diamond for color origin determination. In daylight-equivalent illumination, the diamond was color graded as Fancy brown-pink, but under incandescent light it appeared Fancy purplish gray (figure 4).

When exposed to long-wave UV light at 365 nm, the diamond exhibited medium orange fluorescence. Based on photoluminescence (PL) spectroscopy, collected using several lasers, it was identified as a treated diamond that had been subjected to high-pressure, high-temperature (HPHT) annealing, irradiation, and subsequent low-pressure annealing. The PL spectra were dominated by the presence of strong NV centers at 575 and 637 nm, along with a strong GR1 peak, confirming the cause of the diamond's luminescence as the NV centers.

UV-Vis-NIR absorption spectra were collected at room temperature (figure 5) and at liquid nitrogen temperature inside an integrating sphere for this diamond (along with a 0.48 ct treated pink CVD synthetic that does not show the pronounced color change, for comparison). At liquid nitrogen temperature with the diamond under incandescent illumination, the

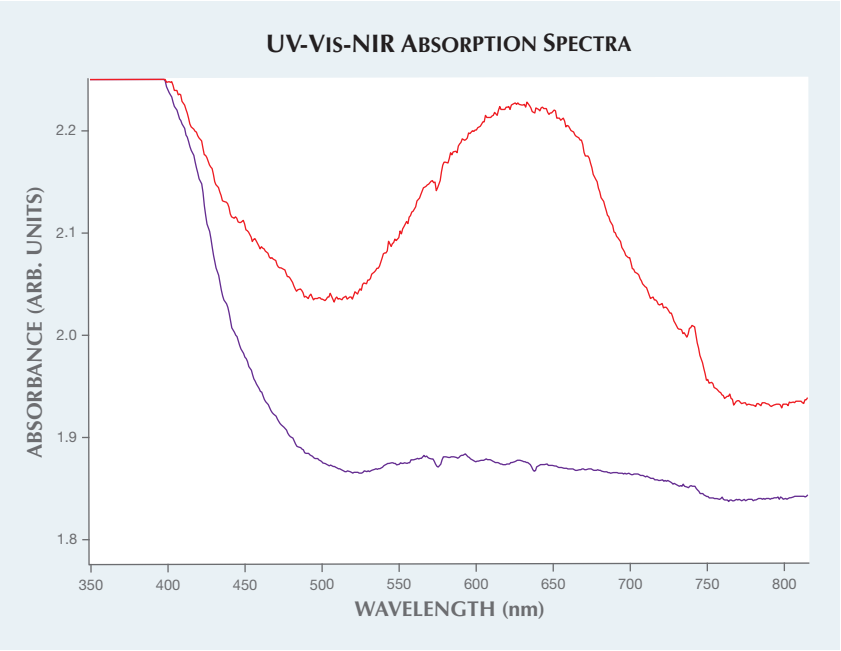

Figure 5. Room-temperature UV-Vis-NIR absorption spectra were collected on the 4.29 ct treated sample (blue trace) and a 0.48 ct treated CVD synthetic (red trace) with a color grade of Fancy Vivid purplish pink. While NV-related red luminescence caused a pronounced difference in color for the 4.29 ct sample, it only produced a minor change in the treated CVD synthetic. In incandescent light (and with minimal influence of the red luminescence), the synthetic's color shifted slightly to Fancy Deep purplish pink. The pronounced absorption from the GR1 peak (550–750 nm) within the 4.29 ct diamond accounts for the purplish gray color in incandescent lighting.

most prominent feature was the GR1 peak creating the purplish gray coloration, comparable to the blue color generated in many irradiated type IIa diamonds. In daylight-equivalent illumination, the emissions of the NV^0 and NV^- centers were superimposed on the absorption spectrum, thus influencing the diamond's color within the yellow to red region of the visible spectrum. Color grading of diamonds includes the effect of fluorescence, and therefore the reported color was Fancy brown-pink.

While treated diamonds have pronounced UV fluorescence due to NV centers, fluorescence spectra collected at a variety of wavelengths show that the NV luminescence is actually stronger when excitation is from blue light (450–500 nm) than from ultraviolet wavelengths, as in the case of this stone (figure 6). This strong emission stimulated by visible light indicates the diamond is colored by red luminescence in response to blue light and, to a lesser extent, by fluorescence due to the UV component in daylight. Other treated pink diamonds, colored by NV absorption, showed similar excitation spectra (Y. Luo and C.M. Breeding, "Fluorescence produced by optical defects in diamond," Summer 2013 *G&G*, pp. 82–97). This red luminescence due to NV centers is comparable to the more commonly noted green transmission luminescence from the H3 centers seen in some yellow diamonds. Such yellow diamonds receive greenish color grades due to the visible influence of the green emission on the perceived color in daylight conditions.

For most treated pink diamonds, red luminescence corresponds with and enhances the pink bodycolor (Fall 2011 Lab Notes, pp. 228–229), much like chromium-related red fluorescence enhances the color of rubies. Since bodycolor closely corresponds to luminescence color for most treated pink diamonds, the color difference between daylight and incandescent light sources is minimal. For example, the 0.48 ct treated pink CVD synthetic diamond (figure 5, red trace) was color graded as Fancy Vivid purplish pink using a daylight-equivalent light and as Fancy Deep purplish pink under an incandescent light. The NV-related emission, excited by the UV to blue light, brightened the diamond in that viewing environment.

The purplish gray bodycolor for this 4.29 ct treated diamond seen under incandescent light derived from the strong GR1 absorption induced by irradiation. The GR1 intensity, as measured by 633 nm photoluminescence spectroscopy and normalized using the diamond Raman peak, was compared with 20 other treated pink diamonds that did not show a substantial color shift. The GR1 intensity of this diamond was 8 times greater than the average value of the 20 treated pink diamonds and 3.5 times greater than the highest value. The GR1 intensity of this diamond was comparable to irradiated green to blue diamonds. In incandescent light, the red luminescence appeared to provide a minimal contribution, as the modifying hue was purplish (implying a reddish component) and not bluish as one might reasonably expect for an irradiated diamond.

Other diamonds have shown a shift in color grade due to appreciable fluorescence. Examples include the 56.07 ct Tavernier diamond, which displays a brown to pink color shift (Y. Liu et al., "The alexandrite effect of the Tavernier diamond caused by fluorescence," *Color Research and Application*, Vol. 23, No. 5, 1998, pp. 323–327), and a few type Ib diamonds with a NV-related color shift from greenish brown to orangy brown (Fall 2011 GNI, pp. 234–235).

Some CVD-grown diamonds also have shown a pink to blue color shift, but due to an entirely different mech-

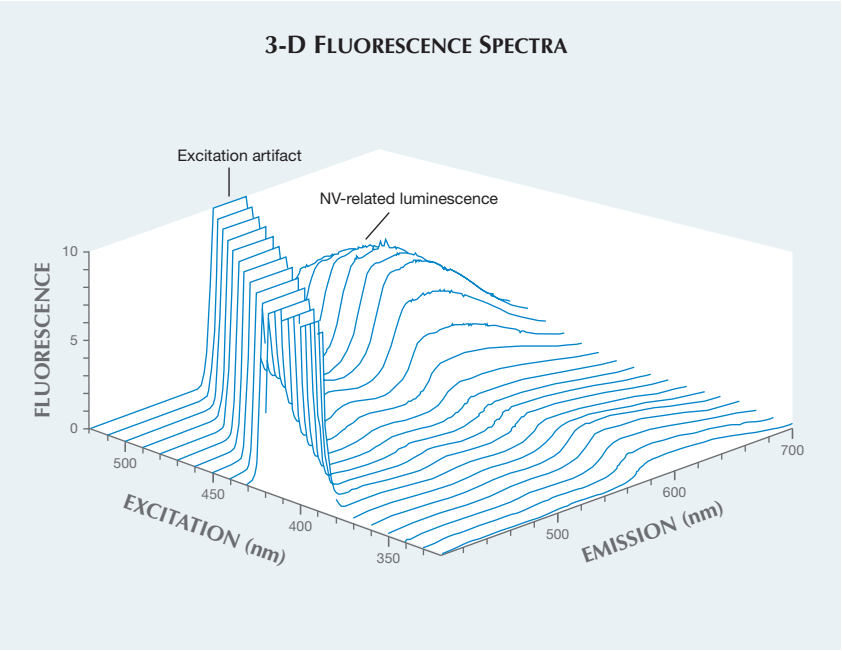

Figure 6. These 3-D fluorescence spectra were collected using excitation from the UV range through the blue range of visible light (320–520 nm). The corresponding fluorescence spectra show that the relative intensity is much higher when excited by wavelengths within the visible region than in the UV region. This indicates that red luminescence excited by visible light is a greater contributor to the pink color than the UV-activated fluorescence. The 0.48 ct treated CVD synthetic shown in figure 5 demonstrated identical behavior—refer to Luo and Breeding (2016) for comparable spectra—and indicates that NV-related luminescence contributes to the graded color in many pink diamonds that are colored by NV centers. The excitation artifact occurs when the emission spectrometer scans across the excitation wavelength.

anism. In those synthetic diamonds, the color change was caused not by a difference in light sources, but by a temporary charge-transfer effect activated by UV exposure. For those CVD synthetics with a high concentration of silicon impurities, UV exposure precipitated a charge transfer between negative and neutral silicon-vacancy centers. In one CVD specimen, the relative concentrations of SiV^- and SiV^0 were essentially reversed with UV exposure and thus influenced the color change from its stable color of Fancy brown-pink to a temporary Fancy Intense blue (U. D'Haenens-Johansson et al., "CVD synthetic gem diamonds with high silicon-vacancy concentrations," *Conference on New Diamond and Nano Carbons*, May 2015, Shizuoka, Japan).

The 4.29 ct natural diamond noted here was HPHT annealed and irradiated to create the NV centers. It appeared to have been irradiated to a far greater extent than most treated pink diamonds, and as a result it had a significantly higher GR1 intensity (as shown in figure 5 and confirmed with 633 nm PL). This accounts for its purplish gray color in incandescent light. The color change between these two attractive colors, along with its large size, makes this diamond quite unusual and serves to illustrate that the color of treated pink diamonds is assisted by red luminescence. This stone also demonstrates that while multiple treatments can provide for some identification challenges, they can also create some truly intriguing products.

Sally Eaton-Magaña

Very Large Artificially Irradiated Yellow Diamond

Artificial irradiation and annealing to enhance or change color is one of the oldest diamond treatments. English chemist Sir William Crookes first discovered the effects of radiation on a diamond's color, conducting experiments using radium salts in 1904. Today, only a very small percentage of all natural diamonds are irradiated, typically with an electron beam. Because of the risk of damage, diamonds subjected to this treatment are typically under 10 carats.

A 59.88 ct yellow diamond (figure 7) recently examined at the New York laboratory received clarity and color grades of SI_1 and Fancy Vivid yellow. While the face-up color distribution was classified as even, we observed a moderate color concentration along the culet typical of some artificially irradiated diamonds (figure 8). Microscopic examination showed noticeable crystal inclusions at 10× magnification as well as extensive burn marks across the entire surface of the stone. The diamond showed chalky blue fluorescence under long-wave UV excitation and medium yellow fluorescence under short-wave UV.

Using a desktop spectroscope, the diamond's visible absorption spec-

Figure 7. This 59.88 ct Fancy Vivid yellow diamond was treated through artificial irradiation and annealing.

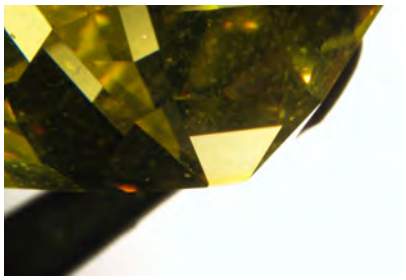

Figure 8. Strong color concentration along the diamond's culet is evidence of artificial irradiation.

trum revealed a series of absorption lines between 415 and 477 nm, indicative of a "cape" diamond. Additionally, an unusually strong peak at 503.2 nm (H3) was noted using a UV-visible spectrometer (figure 9). The enhancement of this H3 center is responsible for the very desirable yellow color. The infrared absorption spectrum showed high concentrations of nitrogen in the one-phonon region, indicating type Ia diamond. Further examination of the infrared region revealed a minor hydrogen defect as well as weak to moderate peaks at approximately 4935 cm^{-1} (H1b) and 5165 cm^{-1} (H1c), further evidence of treatment.

These features led to the conclusion that the diamond was artificially irradiated and annealed (by introducing the H3 defect) to induce a more desirable yellow color. This was by far one of the largest artificially irradiated diamonds identified at GIA, surpassing previous examples by several carats (see Summer 2012 Lab Notes, p. 132; Winter 2014 Lab Notes, p. 295). This diamond reiterates the importance of careful analysis, since even the largest stones may have undergone treatment.

Paul Johnson and Christopher Vendrell

Unusual Purple Inclusion in EMERALD

Depending on geographic locality, inclusions in emerald are typically similar from one stone to the next. We expect to see classic jagged three-phase inclusions in Colombian emeralds or blocky multiphase inclusions and phlogopite in Zambian emeralds, so it is always interesting for the gemologist to observe something out of the ordinary. The Carlsbad laboratory recently examined a 7.11 ct oval mixed-cut emerald (figure 10), identified by standard gemological testing. Microscopic examination revealed jagged to irregular multiphase inclusions, planes of reflective thin films, clarity-enhanced fractures, and—surprisingly—a fairly large purple inclusion with a subhedral form. Upon closer examination, distinct purple and near-colorless banding was visible (figure 11), and the inclusion proved to be singly refractive when viewed between crossed polarizers. The inclusion was too deep within the stone to confirm its identity with Raman spectroscopy, but its appearance and optic character pointed to fluorite. Based on these characteristics, another possible identity could be halite, but this inclusion strongly resembled a color-banded fluorite inclusion previously reported in emerald by GIA's laboratory in 1969. In that example, the surface-reaching inclusion was identified by scraping a sample and analyzing it with X-ray diffraction

Figure 9. The yellow diamond's Vis-NIR absorption spectrum shows a strong peak corresponding to the H3 defect observed at about 503 nm.

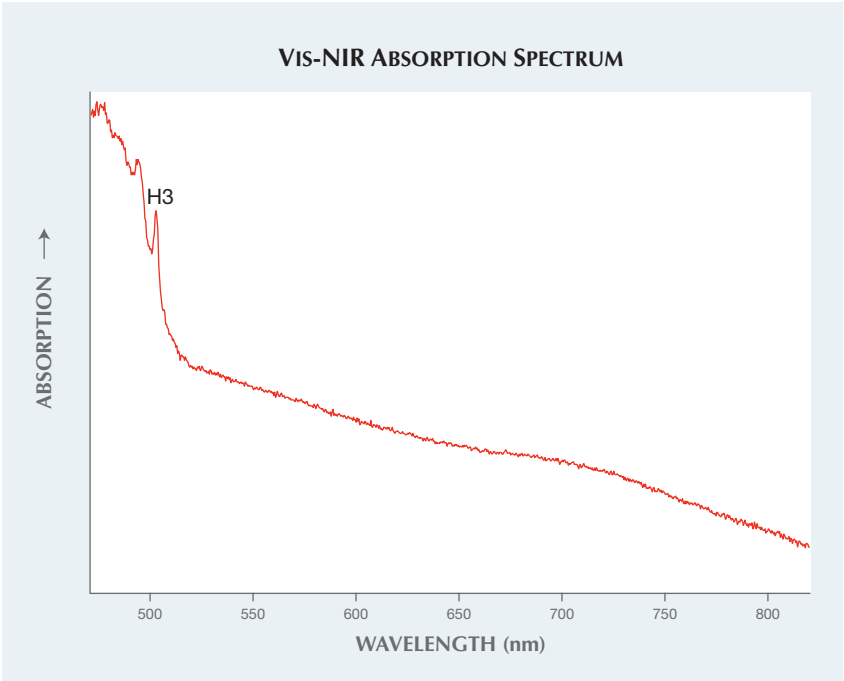

Figure 10. This 7.11 ct emerald contains a large purple inclusion visible under the table.

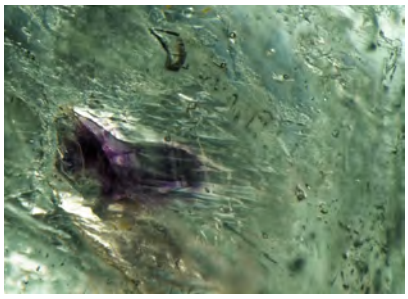

Figure 11. With microscopic examination, clear purple banding is apparent within this fluorite inclusion. Field of view 2.34 mm.

(R.T. Liddicoat, "Developments and highlights at the Gem Trade Lab in Los Angeles," Summer 1969 *G&G*, p. 63).

Fluorite inclusions in emerald have been cited from various localities, as a product of pegmatitic/hydrothermal involvement in formation (E.J. Gübelin and J.I. Koivula, *Photoatlas of Inclusions in Gemstones*, Vol. 3, Opinio Verlag, Basel, Switzerland, 2008, pp. 354–406; D. Schwarz et al., "Emerald and green beryl from Central Nigeria," *The Journal of Gemmology*, Vol. 25, No. 2, 1996, pp. 117–141). These inclusions are usually described as colorless octahedra, although sometimes they are seen as cubes or rounded shapes. Purple banded fluorite is an unusual inclusion in emerald, making this an interesting and unexpected addition to an otherwise typical inclusion scene.

Claire Ito

Non-Nacreous Purple and White PEARLS Reportedly from *Spondylus* Species

The Carlsbad laboratory recently examined three non-nacreous pearls, weighing 7.85 to 9.85 ct and measuring from 10.50 × 10.21 mm to 12.43 × 11.65 × 10.65 mm (figure 12). All three pearls exhibited similar uneven bodycolors and surface characteristics. They displayed purple and white colors with some yellowish brown tints and possessed a porcelaneous surface with mottled to clear fine flames. They were reportedly fished near Ligui, on the eastern coast of the Mexican state of Baja California Sur.

Similar surface structures have been reported in *G&G* (Fall 2014 Lab Notes, pp. 241–242; Winter 2015 Lab Notes, pp. 436–437; Summer 2016 Micro-World, pp. 202–203). A characteristic reflective blue coloration on the base of the 9.85 ct semi-baroque button (figure 13) was clearly visible when the flame structure was illuminated with a fiber-optic light. Moreover, subsurface to surface-reaching acicular inclusions found in most *Spondylus* pearls examined previously were also present in these samples. These inclusions, which appear in the form of tubes or needles, are often associated with the flame structure. At first the inclusions were believed to be parasite channels, which are sometimes observed in shells and pearls of various nacreous and non-nacreous mollusks. But after careful inspection they were seen to be part of the structure, radiating from within and reaching the surface in the same direction and with fairly consistent size and shape—whereas the parasite channels are irregularly shaped and in various sizes, running in random directions and usually crossing over each other.

The pearls' dimpled surface texture appears to be caused by the slightly recessed openings where these inclusions reach the surface. This unique feature is also found on the interior of *Spondylus* shells in GIA's Bangkok laboratory collection (figure 14). The resemblance between a pearl's surface and the interior surface of its host are useful in identifying the mollusk species. Yet many marine gastropods and bivalves pro-

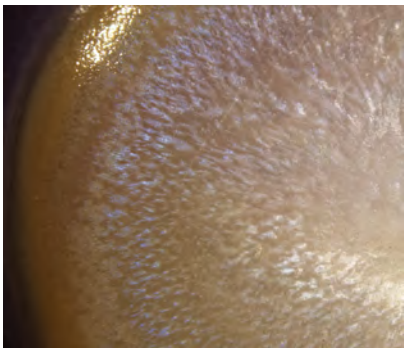

Figure 13. The characteristic reflective blue coloration of Spondylus *pearls was visible within the flame structure of the semi-baroque button pearl when illuminated with a fiber-optic light. Field of view 5.77 mm.*

Figure 12. These three purple and white non-nacreous pearls weighing 7.85, 8.37, and 9.85 ct (left to right) are reportedly from Spondylus calcifer.

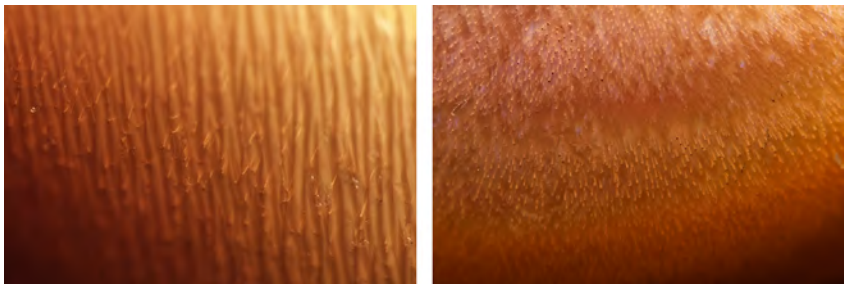

Figure 14. Subsurface to surface-reaching acicular inclusions were found on the interior of a Spondylus *shell (left) from the GIA Bangkok reference collection and associated with the flame structure in a* Spondylus *pearl (right). Fields of view 1.31 mm and 2.37 mm, respectively.*

duce non-nacreous pearls, and their similar surface structure and color sometimes make mollusk identification challenging. As with the previously reported *Spondylus* pearls, microradiography of all three pearls revealed tight structures, and no obvious growth arcs were seen.

The *Spondylus* genus (commonly known as "thorny" or "spiny" oyster) consists of about 76 living species distributed in tropical waters around the world. *Spondylus princeps* and *Spondylus calcifer* (also known as *Spondylus limbatus*) are two of the main species on the western coast of the Americas. *S. princeps* is found from the gulf side of Baja California down the Pacific coast of Mexico through Panama to northwest Peru. *S. calcifer* is found in the Sea of Cortez (Mexico) and Ecuador (K. Lamprell, *Spiny Oysters: A Revision of the Living Spondylus Species of the World*, Jean Lamprell, Brisbane, Australia, 2006). Most *Spondylus* pearls examined by GIA are reportedly from *Spondylus princeps*, whose bodycolor is typically white to cream or various saturations of pink, orange, and brown. This is the first time GIA has examined pearls with such a dominant purple hue reported to be from *Spondylus calcifer*. This species has been recorded as producing pearls in Costa Rica (E. Strack, *Pearls*, Ruhle-Diebener-Verlag GmbH & Co., Stuttgart, 2006, p. 59).

Artitaya Homkrajae

Lead Glass–Filled Black Star SAPPHIRE

Fracture and cavity filling of gemstones has been practiced for hundreds of years. In recent times, this treatment has become more sophisticated and widespread, particularly with the use of lead glass, which is most often seen in rubies. The addition of lead oxide (PbO) to silica glass lowers its working temperature and viscosity while raising its refractive index from approximately 1.5 to as high as 1.8. Thus, the filler has an RI that matches many gem materials, making fractures and voids virtually disappear. But the softness and low melting point of the filler create durability issues, especially in low-quality filled rubies (S.F. McClure et al., "Identification and durability of lead glass–filled rubies," Spring 2006 *G&G*, pp. 22–34).

Common inclusion features for lead glass–filled ruby composites include blue flashes from the fractures and trapped gas bubbles. Glass features can also be detected using Fourier-transform infrared (FTIR) spectrometry and energy-dispersive X-ray fluorescence (EDXRF) spectroscopy. But if the ruby has very few areas that are enhanced with lead glass, they may not be obvious under magnification, and FTIR and EDXRF may not detect them. Real-time X-ray (RTX) imaging systems, used by GIA to identify pearl growth features and confirm filling in diamonds, can be beneficial in differentiating between lead glass and ordinary glass filling in rubies and other gemstones. This is due to opacity differences, as lead glass has a lighter appearance than glass without lead. A combination of X-ray imaging and magnification is also capable of quantifying the extent of lead glass treatment performed on a gemstone.

A 25.10 ct opaque black star sapphire (figure 15) was submitted to the New York laboratory for identification. The stone contained a few hairline fractures and dense golden silk needles. At first glance, the sapphire had a few features that would arouse suspicion for treatment, such as round cavities on the base and a few inconspicuous fractures (figure 16). The sapphire also had a specific gravity of 4.04, which is above the normal range for corundum. Natural black sapphire may have a higher SG due to abundant asterism-causing inclusions of rutile or hematite, both of which are denser than corundum. Because of the stone's opacity, it was difficult to observe internal inclusions under magnification.

Using X-ray imaging analysis (figure 17), it was clear that the fractures and multiple cavities had been filled

Figure 15. This 25.10 ct black star sapphire was enhanced with lead glass.

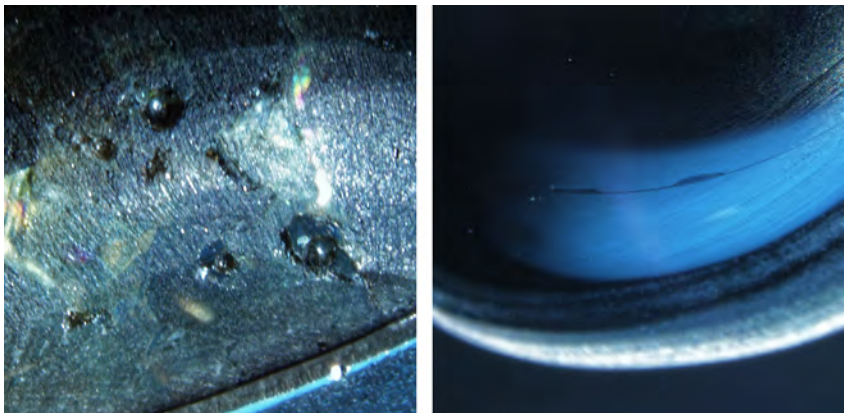

Figure 16. Gas bubbles visible in the sapphire's cavities (left) and a thin fracture with different surface luster (right) indicate the possibility of lead glass filling. Fields of view 2.10 mm (left) and 3.90 mm (right).

with lead glass, and this finding was confirmed by EDXRF. These properties would have been extremely difficult to see under normal visual magnification.

This is the first example of a lead glass–filled black star sapphire examined in the New York laboratory.

Akhil Sehgal

Figure 17. Face-up (top) and profile (bottom) RTX images of the black star sapphire. The white areas indicate higher opacity in fractures and cavities, evidence of lead glass filling. Noticeable round gas bubbles are trapped in cavity fillings.

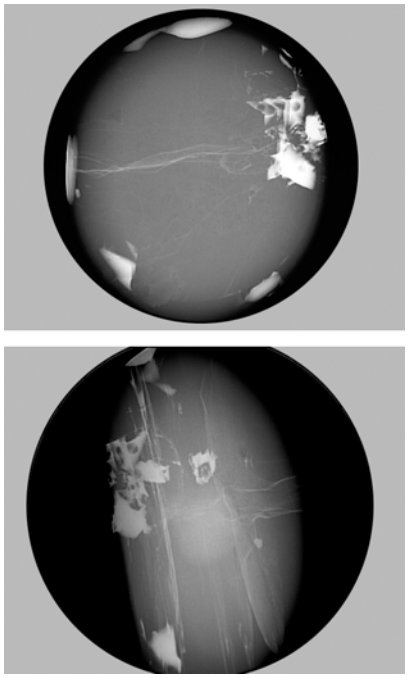

Sapphire Rough Filled with Green Lead Glass

The Carlsbad laboratory recently examined a yellow-green hexagonal prismatic crystal (figure 18, left) that was presented as sapphire. The rough specimen was approximately 11 mm long. The specific gravity was measured as 4.00, and the stone was inert to both long- and short-wave UV. The identity of the rough sapphire was confirmed by Raman spectroscopy.

Microscopic examination revealed that the stone was partially covered by drops of green glassy residue, and numerous fractures throughout it were filled with the same material. Also observed were numerous trapped gas bubbles and a prominent orange flash effect, consistent with a lead-glass filling (figure 18, right). Energy-dispersive X-ray fluorescence (EDXRF) analysis confirmed the presence of lead.

Laser ablation–inductively coupled plasma–quadrupole mass spectrometry (LA-ICP-MS) was used to investigate the chemical composition of the green glassy residue. A line of ablation spots, positioned on one of the flat crystal faces, was designed to cross a large drop of the residue. The oxide weight percent profile (figure 19, left) revealed that the residue contained 9.3 to 9.7 wt.% B_2O_3, 23.7 to 24.9 wt.% Al_2O_3, 12.2 to 12.6 wt.% SiO_2, 3.6 to 4.2 wt.% CuO, 1.2 to 1.3 wt.% CdO, and 45.4 to 47.4 wt.% PbO. The combined oxide weight percent of Li, Na, K, Ca, and Zr was around 1.5 (averaged value). The chemical analysis confirmed that the filler was lead glass.

With such a small amount of Al (2.6 wt.% Al_2O_3) in the lead glass (Z.Q. Zeng and P. Hing, "Preparation and thermal expansion behavior of glass coatings for electronic applications," *Material Chemistry and Physics*, Vol. 75, No. 1–3, 2002, pp. 260–264), the approximate composition of major elements can be obtained by subtracting 24.22 wt.% Al_2O_3 (arising from the host sapphire crystal) from the total chemical composition and renormalizing the sum

Figure 18. Left: This hexagonal green sapphire rough was treated with a green lead-glass filling. Right: Green residue and trapped gas bubbles are seen in the filled fractures; field of view 2.90 mm.

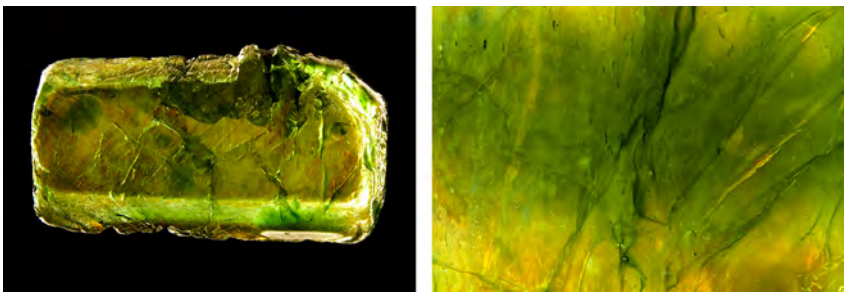

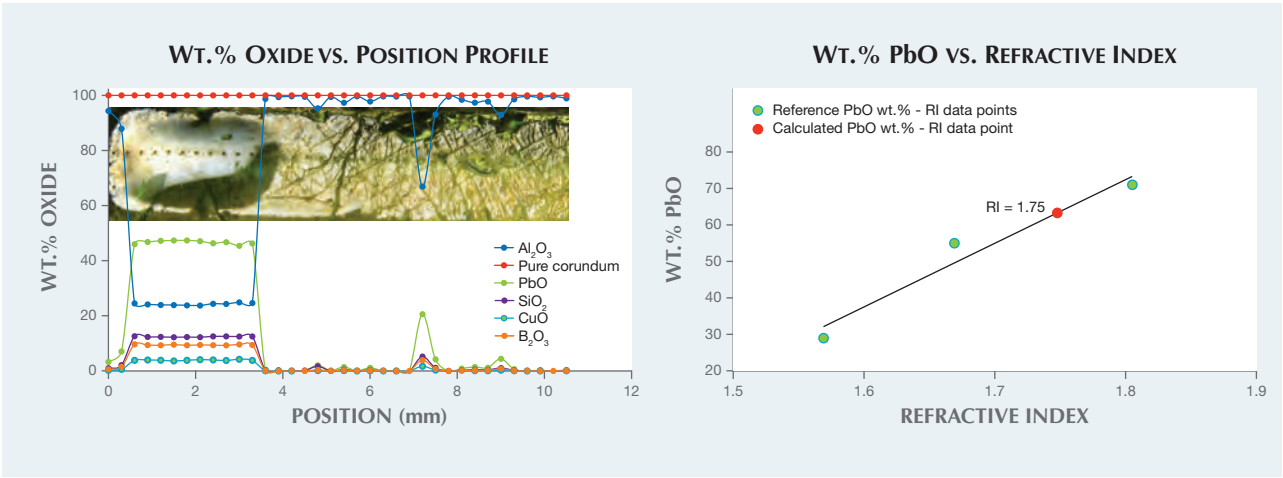

Figure 19. Left: The wt.% oxide profile shows a strong correlation between the glassy residue and a high Pb concentration. Right: The lead glass shows a refractive index of 1.75 for a PbO content of 63.3 wt.%.

to 100 wt.% oxide (R. Barbour, *Glass-blowing for Laboratory Technicians*, Wellington, New Zealand, Pergamon Press, 1978, p. 4). The renormalized composition of the lead glass was 63.3 wt.% PbO, 16.9 wt.% SiO_2, 12.8 wt.% B_2O_3, 5.3 wt.% CuO, and 1.7 wt.% CdO. The PbO wt.% was plotted on the Pb wt.% oxide vs. refractive index plot (http://physics.info/refraction) and showed an RI of 1.75, which is very close to corundum's RI of 1.76–1.77 (figure 19, right). The high refractive index of the glass concealed the difference in luster between corundum and filler.

A previous study reported on blue cobalt-colored lead glass–filled sapphires whose color was assigned to the presence of a small amount of cobalt in the filler (T. Leeawatanasuk et al., "Cobalt-doped glass-filled sapphire; an update," *Australian Gemmologist*, Vol. 25, No. 1, 2013, pp. 14–20). The green color of the glass in this specimen was likely caused by the combination of CuO (which causes a greenish blue color in glass) and CdS (which causes a yellow color; see B.H.W.S. De Jong et al., "Glass," in *Ullmann's Encyclopedia of Industrial Chemistry*, Wiley-VCH, 2000, http://dx.doi.org/10.1002/14356007.a12_365). The yellowish appearance and the high levels of Fe (1629 to 2640 ppmw) in the area without filler indicate that the piece might have been a yellow sapphire before being filled. This was the first sapphire with green lead-glass filling examined at the Carlsbad laboratory.

Ziyin Sun and Jonathan Muyal

SYNTHETIC DIAMONDS

Large Crystal Inclusion in CVD Synthetic Diamond

Most inclusions in CVD synthetic diamonds are particulate or needle-like, and they tend to be confined to a plane (Spring 2013 Lab Notes, pp. 47–49). A previous report covered a case where the inclusions were scattered throughout in a random pattern (Fall 2014 Lab Notes, pp. 238–239), but even these inclusions were flat or pinpoint-sized. A 0.90 ct transparent colorless round brilliant CVD synthetic diamond was found to have an unusually large compact opaque black crystal inclusion. This 302.3 µm inclusion (figures 20 and 21) placed it in the SI clarity range and, as seen in the images, was significant in size in all three dimensions, unlike the usual geometry of CVD growth remnants. The inclusions that exist in a flat plane are thought to be related to imperfections at the growth surface, and the plane of inclusions will generally

Figure 20. This 302.3 µm graphite inclusion encircled by tension fissures was observed in a CVD synthetic diamond. Subtle iridescent colors resulting from strain were also visible around the inclusion in polarized light. Field of view 1.42 mm.

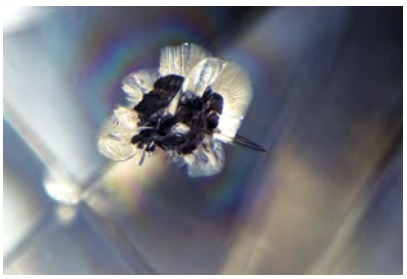

Figure 21. The large graphite crystal and its radiating tension halo, viewed from the side through the pavilion. Field of view 1.42 mm.

line up with a growth plane seen in DiamondView images. DiamondView imaging of this specimen showed no growth layers, only the dislocation networks characteristic of CVD synthetic diamonds.

The inclusion was most likely carbon in the form of graphite, although attempting to collect a Raman spectrum on it yielded no results. The inclusion was surrounded by stress fractures; it is unknown whether these were induced during the growth process or resulted from a post-growth treatment. Polarized illumination also revealed some iridescent color due to strain surrounding the inclusion. This sample was graded in the colorless range; this was a sign of post-growth treatment, as most CVD synthetics are brownish from the growth process (the treatment was confirmed by the absence of the 596/597 nm doublet in the photoluminescence spectra).

Under microscopic examination, this inclusion bore a strong resemblance to an inclusion one would find in a natural diamond. Since the size and structure are very different from anything previously seen in a CVD synthetic, identification based on these properties alone could lead to confusion. Luckily, Fourier-transform infrared (FTIR) spectroscopy revealed that the specimen was type IIa, an indication that a diamond may be synthetic (CVD or HPHT). Synthetic origin was proven by DiamondView images revealing growth patterns characteristic of CVD growth and large silicon-vacancy peaks detected by photoluminescence spectroscopy. It is therefore prudent to undertake all testing needed to conclusively separate natural and synthetic diamonds.

Troy Ardon and Jonathan Muyal

Screening of HPHT Synthetic Melee With Natural Diamonds

Significant amounts of melee-size synthetic diamonds produced by both HPHT and CVD technologies are manufactured for the jewelry industry. The "salting" of natural diamond melee parcels with HPHT-grown synthetic melee is seen more frequently in the trade today. This presents a threat to the integrity of diamond dealers and manufacturers who might unknowingly sell or use synthetic diamonds and represent them as natural. In response, GIA has introduced a melee analysis and screening service aimed at helping the trade combat this problem. The screening is rapid and relatively inexpensive. This service can screen large quantities of diamond melee and separate natural diamond from synthetic material (both HPHT and CVD grown), natural HPHT-processed diamond, and diamond simulants such as cubic zirconia or moissanite. In addition, a color grade within the D–Z range can be assigned to each diamond.

In August 2016, a group of 3,005 melee with a total weight of 70.56 carats (figure 22) was submitted to GIA's New York lab for screening service. Initial testing using our fully automatic screening device, which is based on spectroscopic methods, passed 2,969 (98.7%) of them as natural diamond. Of the remaining 36, 12 were subsequently identified as natural material by methods including photoluminescence (PL) spectroscopy, and only 24 were referred for further testing to confirm their identity as natural, treated, or synthetic diamond.

Figure 22. This parcel of 3,005 melee diamonds with a total weight of 70.56 carats was submitted for analysis.

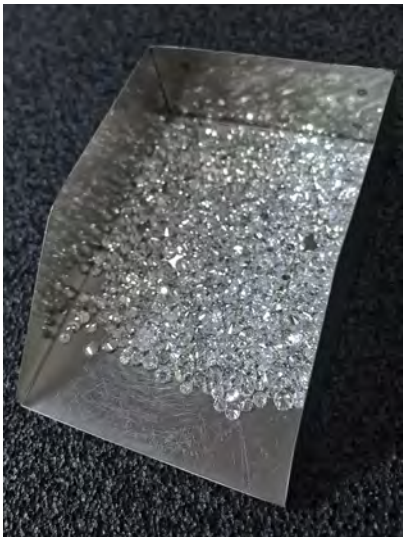

Figure 23. From an initial screening of 3,005 melee diamonds, 24 specimens were referred for further testing. Of these, three were HPHT-grown synthetic diamonds.

Additional testing with Fourier-transform infrared (FTIR) absorption spectroscopy, Raman PL spectroscopy, and fluorescence imaging techniques identified 21 of these 24 melee as natural diamond. This analysis also confirmed that three (0.1%) of the melee in the parcel were HPHT-grown synthetic diamonds (figure 23).

This highlights the practice of "salting" parcels of natural diamond melee with a small percentage of synthetic diamond melee, and the importance of advanced testing to identify them.

Ivana Petriska Balov and Paul Johnson

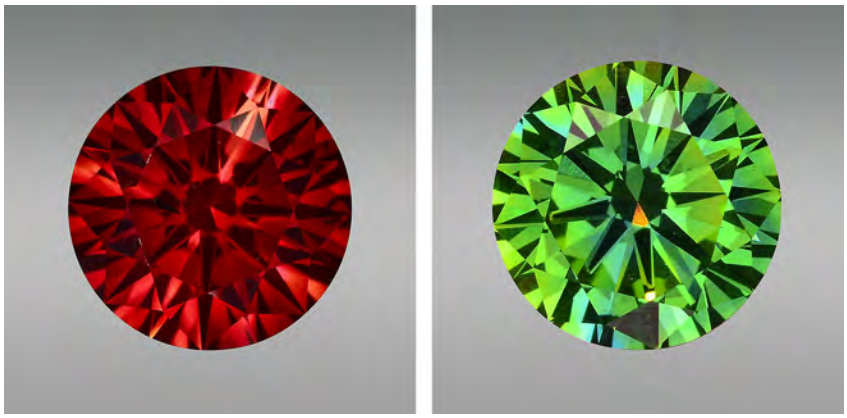

Figure 24. These two treated synthetic diamonds, a 0.57 ct Fancy red and a 0.50 ct Fancy Vivid yellowish green, show strikingly vibrant colors rarely found in natural-color diamonds.

Figure 25. A large metallic inclusion breaks the table of the Fancy red synthetic diamond. This inclusion and the tiny pinpoint clouds in the background are typical identification features of HPHT synthetics. Field of view 2.85 mm.

Treated Red and Green HPHT SYNTHETIC DIAMONDS

Natural-color red and green diamonds are extremely rare and command some of the highest prices in the market. Only a small number of natural diamonds have ever been graded as Fancy red without any modifying hues such as brownish red or orangy red. A 0.57 ct round brilliant with Fancy red color (figure 24, left) was recently submitted to GIA's New York laboratory for a colored diamond grading report. It showed a heavily saturated and pure red color, without any modifications to the red hue. From another client, we received a 0.50 ct round brilliant graded as Fancy Vivid yellowish green (figure 24, right) for a synthetic colored diamond grading report. The striking features shared by these two specimens caught our attention.

Examination with a standard gemological microscope revealed that both of them contained pinpoint clouds and metallic inclusions (figure 25), a typical feature of synthetic diamonds grown by high pressure and high temperature (HPHT). Mid-FTIR absorption spectra identified both as type Ib, with the relatively high concentration of isolated nitrogen that is responsible for the yellow to brown color typically observed in HPHT synthetics (Winter 2015 Lab Notes, pp. 430–431).

The strong short-wave UV radiation of the DiamondView (figure 26) showed red and yellowish green fluorescence in the red and green samples, respectively. Furthermore, the presence of both cubic {100} and octahedral {111} growth sectors in the DiamondView images suggested that the specimens formed with a relatively high growth rate that facilitated cubic and octahedral development simultaneously, a strong indicator of synthetic origin (Winter 2015 Lab Notes, pp. 429–430).

Diffused lighting showed uneven color zoning in both samples, consisting of their bodycolors and the yellow color from the isolated nitrogen content (figure 27). Spectroscopic analysis revealed that the Fancy red synthetic had an unusually strong peak at 637 nm (NV^- center). This peak indicates color alteration by post-growth annealing (T.W. Overton and J.E. Shigley,

Figure 26. DiamondView fluorescence images of the Fancy Vivid yellowish green synthetic diamond (left) and the Fancy red synthetic diamond (center and right) show similar combinations of cubic and octahedral sectors.

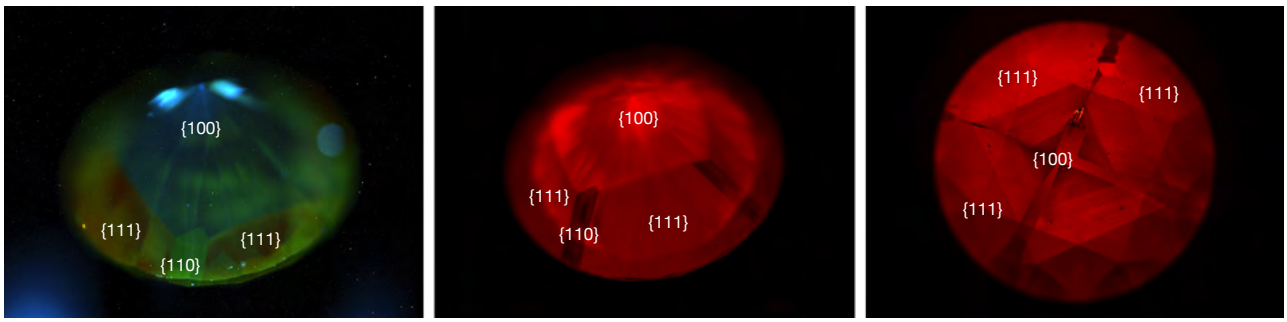

Figure 27. Under polarized light, the Fancy Vivid yellowish green synthetic diamond (left) displays patchy yellow color zoning caused by isolated nitrogen and a green color concentration on the culet caused by post-growth artificial irradiation treatment. The Fancy red sample (right) shows yellow to near-colorless zones following the cubic growth sectors, with the red color caused by post-growth annealing. Fields of view 7.19 mm (left) and 4.79 mm (right).

"A history of diamond treatments," Spring 2008 *G&G*, pp. 33–55). In the Fancy Vivid yellowish green synthetic, a concentration of green color on the culet area indicates that artificial irradiation was applied to alter the as-grown yellow color to vivid green.

Both synthetic diamonds underwent post-growth treatment to change their color to the desirable red and yellowish green hues. While the yellowish green round brilliant received a synthetic colored diamond report, the undisclosed nature of the Fancy red's growth required the lab to issue an identification report to properly disclose its synthetic origin.

Yixin (Jessie) Zhou and Paul Johnson

PHOTO CREDITS:
Troy Ardon—1; Robison McMurtry—4; Jian Xin (Jae) Liao—7, 15, 23, 24; Christopher Vendrell—8; C.D. Mengason—10; Jonathan Muyal—11, 18, 19 (inset), 20, 21; Robert Weldon—12; Artitaya Homkrajae—13, 14 (left); Moqing Lin—14 (right); Akhil Sehgal—16; Ivana Petriska Balov—22; Yixin (Jessie) Zhou—25, 26, 27.

For online access to all issues of GEMS & GEMOLOGY from 1934 to the present, visit:
gia.edu/gems-gemology